

Hot-air balloon as a platform for boundary layer profile measurements during particle formation

Lauri Laakso¹⁾, Tiia Grönholm¹⁾, Liisa Kulmala²⁾, Sami Haapanala¹⁾, Anne Hirsikko¹⁾, Edward R. Lovejoy³⁾, Jan Kazil⁴⁾, Theo Kurtén¹⁾, Michael Boy¹⁾, E. Douglas Nilsson⁵⁾, Andrey Sogachev¹⁾, Ilona Riipinen¹⁾, Frank Stratmann¹⁾⁶⁾ and Markku Kulmala¹⁾

¹⁾ Department of Physical Sciences, P.O. Box 64, FI-00014 University of Helsinki, Finland

²⁾ Department of Forest Ecology, P.O. Box 27, FI-00014 University of Helsinki, Finland

³⁾ NOAA Aeronomy Laboratory 325 Broadway, Boulder, CO 80303, USA

⁴⁾ NOAA Earth System Research Laboratory, 325 Broadway, Boulder, CO 80305, USA

⁵⁾ Department of Applied Environmental Research, Stockholm University, SE-10691 Stockholm, Sweden

⁶⁾ Institute for Tropospheric Research, Permoserstrasse 15, D-04318 Leipzig, Germany

Received 21 Dec. 2006, accepted 7 Mar. 2007 (Editor in charge of this article: Veli-Matti Kerminen)

Laakso, L., Grönholm, T., Kulmala, L., Haapanala, S., Hirsikko, A., Lovejoy, E. R., Kazil, J., Kurtén, T., Boy, M., Nilsson, E. D., Sogachev, A., Riipinen, I., Stratmann, F. & Kulmala, M. 2007: Hot-air balloon as a platform for boundary layer profile measurements during particle formation. *Boreal Env. Res.* 12: 279–294.

In this study, we used a hot-air balloon as a platform for boundary layer particle and cluster measurements. We did altogether 11 flights during the springs of 2005 and 2006. During the spring of 2006, we observed five new-particle formation days. During all days, new-particle formation took place in the mixed boundary layer. During one of the days, we observed particle formation in the free troposphere, separate from that of the mixed layer. The observations showed that the concentration of freshly-formed 1.5–2 nm negative ions was several times higher than the concentration of positive ions. We also clearly observed that nucleation during one of the days, 13 March 2006, was a combination of neutral and ion-induced nucleation. During some of the days, particle growth stopped at around 3 nm, probably due to lack of condensable organic vapours. Simulations of boundary layer dynamics showed that particles are formed either throughout the mixed layer or in the lower part of it, not at the top of the layer.

Introduction

An important phenomenon associated with the atmospheric aerosol system is the formation of new atmospheric aerosol particles. Atmospheric aerosol formation consists of a complicated set of processes that include the production of nanometer-size clusters from gaseous vapours, the growth of these clusters to detectable sizes,

and their simultaneous removal by coagulation with the pre-existing aerosol particle population (e.g. Kerminen *et al.* 2001, Kulmala 2003). Once formed, aerosol particles need to grow further to sizes > 50–100 nm in diameter until they are able to influence climate, even though smaller particle may have influences on human health and atmospheric chemistry. While aerosol formation has been observed to take place almost every-

where in the atmosphere (Kulmala *et al.* 2004a), serious gaps in our knowledge regarding this phenomenon still exist. These gaps range from the basic process-level understanding of atmospheric aerosol formation to its various impacts on atmospheric chemistry, climate, human health and environment. Most of the studies reviewed by Kulmala *et al.* (2004a) are based on aerosol particle size distribution measurements at the Earth's surface, and the results have been generalized to represent the whole planetary boundary layer (BL).

There are only few studies which focus on the vertical extent of BL nucleation. Hoppel *et al.* (1994) measured particle formation in a marine BL with a small zeppelin accommodating several instruments for the measurement of gases, meteorology and aerosol particles. They measured the aerosol particle size distribution down to 5 nm, and detected several particle formation events in the mixed boundary layer. To explain the results, the authors suggested that nucleation may take place on pre-existing neutral or ion clusters.

Stratmann *et al.* (2003) measured vertical profiles of meteorological variables, together with the concentration of SO₂ and the number concentration of 5–10 nm particles, during several nucleation bursts in the continental BL. They found that particle formation took place separately in the mixed layer (ML) and in the residual layer (RL). Siebert *et al.* (2004) found high particle concentrations in the size range 5–10 nm which were de-coupled from the particle concentrations at ground level, suggesting a nucleation event near the inversion layer.

Typical time scales of mixing inside the BL are less than half an hour (Hoppel *et al.* 1994, Nilsson *et al.* 2001). For nucleated particles, it might take several hours to grow to 5 nm size (e.g. Kulmala *et al.* 2004a, 2004b), since the growth rates of sub 5 nm particles are typically 1–2 nm h⁻¹. Thus, measurements of 5 nm particles can not necessarily provide information on the location of the initial nucleation process inside a specific layer (e.g. ML or RL).

In this study, we aim to observe freshly-nucleated particles throughout the BL, and in particular to find out new information on the probable location of atmospheric new particle formation.

For that purpose, we measured vertical profiles with several instruments using a hot-air balloon as a measurement platform. Especially, we utilized an Air Ion Spectrometer (AIS) (Mirme *et al.* 2007) to perform ion measurements down to 1.5 nm. The measurements were carried out in April 2005 and March 2006, but due to the lack of particle formation events in spring 2005, we present here data from spring 2006 only.

In this article, we first discuss several processes which may facilitate or prevent nucleation in the BL. Next, we describe our ground-based measurements, discuss the applicability of a hot air balloon as a measurement platform and introduce the instrumentation placed in the gondola. After that, we briefly describe our BL modeling approach. The results section consists of detailed studies of several specific days and an overview of the observation results. In the next section, we discuss the possible explanations for, and consequences of, our results.

Processes favoring or preventing nucleation in the boundary layer

Figure 1 summarizes the important phenomena which can facilitate or prevent nucleation in the BL. An excellent overview on different processes and earlier observations is given by Hellmuth (2006a, 2006b, 2006c, 2006d). A few alternatives have been suggested for the altitude that would be the most favorable place for nucleation: (1) just above or even inside the canopy, (2) at the height of maximum turbulence, and (3) at the top of the boundary layer. Nucleation can also occur inside the whole BL.

Near the surface, concentrations of several vapours which can contribute to particle growth are higher than in the residual layer or in the free troposphere. This applies especially to organic condensable vapours, the precursors (isoprene, monoterpenes and sesquiterpenes) of which are emitted by trees. Also, the relative humidity is usually lower than at higher altitudes, and this may favor some processes related to organic chemistry (Hyvönen *et al.* 2005).

Turbulence (eddy diffusivity, mixing strength; see Stull 1988) reaches its maximum at about one third of the mixed layer height. Nilsson *et al.*

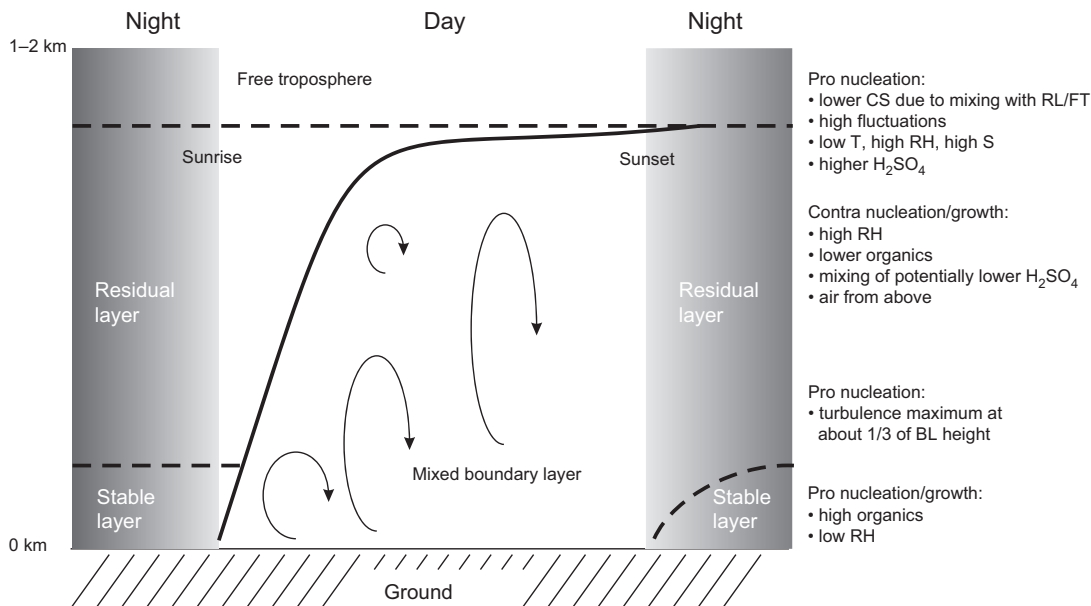


Fig. 1. Factors affecting new particle formation in a boreal forest boundary layer.

(1998) suggested that turbulent mixing together with other mixing processes increases nucleation rates (*see also Siebert et al. 2004*). This is mainly due to the fact that high turbulence also leads to high fluctuations. Sometimes, the concentration maxima due to spatial and temporal variations are so high that nucleation or activation of clusters will start.

The top of the boundary layer may also be a favorable place for nucleation due to several processes. Because of the adiabatic cooling of lifting air parcels, the lowest temperatures in the mixed layer are at the top of the layer. Lower temperatures lead to higher saturation ratios of nucleating vapours which, according to e.g. classical nucleation theory, enhances nucleation (e.g. Lovejoy *et al. 2004*). Other enhancing phenomena are high fluctuations in, for example, wind velocity, temperature and saturation, together with large gradients and a lower pre-existing particle surface due to the mixing of cleaner air from the residual layer. On the other hand, some variables may also prevent nucleation at the top of the boundary layer. These include the higher relative humidity (Hyvönen *et al. 2005*) and lower concentrations of nucleating and condensing vapours. The issue of the effect of a high relative humidity in our conditions is contra-

dictory. According to nucleation theories water vapour should assist nucleation (e.g. Lovejoy *et al. 2004*), whereas our data-mining study shows that a high relative humidity hinders new-particle formation (Hyvönen *et al. 2005*).

In principle, both activation of ion or neutral clusters (Kulmala *et al. 2000*, Kulmala *et al. 2006*) and nucleation will be possible in all layers. Therefore, it is difficult to predict where in the boundary layer nucleation actually takes place based on theoretical methods alone. However, it is somewhat easier to see from measurements which layer is the most favourable for new-particle formation.

Measurements

Ground-based measurements

The aim of our campaign, conducted between 10 and 17 March 2006 was to measure vertical aerosol particle and negative and positive air ion concentration profiles during nucleation events. The starting point of measurements was a football field 400 meters west from the SMEAR II station (Station for Measuring Forest Ecosystem–Atmosphere Relations), which is located

in southern Finland (61°51'N, 24°17'N, 181 m above the sea level). The SMEAR II station was designed to study mass and energy fluxes in the atmosphere–vegetation–soil continuum (Kulmala *et al.* 2001, Hari and Kulmala 2005). Continuous measurements of the concentrations of NO, NO_x, SO₂, O₃, H₂O, CO₂ and CO, of the fluxes of CO₂, H₂O and aerosol particles, of the number size distribution of aerosol particles as well as of meteorological data (temperature, pressure, radiation, wind velocity and direction) have been conducted since 1996. The wind velocity profile measurements are carried out by sound detection and ranging (SODAR). The measurements of gas concentrations and meteorological data are performed at different height levels: 4.2, 8.4, 16.8, 33.6, 50.4 and 67.2 meters on the measurement tower. The number size distribution of aerosol particles is measured at 2-m height by two differential mobility particle sizers (DMPS). The first device classifies particles between 3 and 10 nm and the second between 10 and 500 nm (Aalto *et al.* 2001). Ion size distributions have been measured since March 2003.

We also utilized a special type of DMPS called an ion-DMPS. The ion-DMPS provides the charging state of nucleation mode particles compared to the equilibrium charge distribution. If the nucleation mode particle population carries more charges than a particle population at charging equilibrium, the particles are overcharged, if less, then they are undercharged (Laakso *et al.* 2007).

The area belongs to the southern boreal zone, and the forest consists mainly of coniferous trees. Like 56% of the forest area in southern Finland, the dominating species in the area is Scots pine. The nearest cities are Ruovesi (25 km north), Orivesi (20 km south), Jämsä (50 km northeast) with about 5000, 10 000 and 15 000 inhabitants, respectively, and Tampere (50 km southwest), with 200 000 inhabitants.

Balloon measurements

For vertical profile measurements, we used a hot-air balloon as platform. This is not a new idea: since the first hot-air balloon flight in France in 1783, balloons have been used for

scientific purposes like atmospheric and human physiology studies. Nowadays, hot-air balloons have mainly been supplanted by aircraft. However, there is an advantage in using hot-air balloons in atmospheric measurements. The balloon is carried along by the wind, and thus the effects of advection and horizontal heterogeneity do not play a big role in the measurements. Also, the descent speed is only 2–5 m s⁻¹, which makes the use of measurement devices with response times up to 30–60 seconds possible. The low vertical velocity also allowed us to measure smaller scale phenomena than what would be possible for example with an airplane. If the velocity of a plane is 100 m s⁻¹, a one-minute time resolution corresponds to a spatial scale of several kilometers. Thermals, for example, have a scale of only a few hundred meters. An additional advantage of a hot-air balloon is that measurement instruments do not need to be modified for rapid pressure differences as in the case of airplanes.

The hot-air balloon we used in this study was an Ultramagic S-130 with an Ultramagic C-6 gondola. The volume of the envelope was about 3700 m³ (height 23.5 m and equator diameter 20.5). The burner, an Ultramagic MK-21 double burner, was fueled by propane.

The burner of the balloon causes contamination during ascents, which can be clearly seen from the measured aerosol particle and carbon dioxide concentrations. To avoid contamination, we placed our 3-m-long main inlet (the diameter of 10 cm) with a high flow rate (several meters per second) about 2 m below the gondola base. In addition, we used only data which we measured during descent of the balloon, when the use of the burner is minimal and we get a flow of clean air below the gondola. The results show that during descent we did not get any contamination. The balloon was equipped with several instruments, which are shortly described below.

We used two TSI-3007 condensation particle counters to measure the aerosol particle total number concentration (Model 3007 Condensation Particle Counter, TSI Inc.). One of them was in the gondola, measuring through the main inlet, and the other one was placed below the gondola base. According to the manufacturer's specifications, the TSI-3007 is capable of measuring particle total number concentrations up to 10⁵ cm⁻³,

with a lower detection limit of 10 nm. The operation temperature range is given as 10–35 °C. However, we made laboratory tests to check the device's ability to measure under lower temperatures and a decreased pressure of 850 hPa, which corresponds to conditions at the altitude of about 1500 m (T. Grönholm unpubl. data). According to the laboratory measurements, the TSI-3007 is capable of functioning under the temperature and pressure conditions that were encountered in this study.

We used a Licor LI-7500 open path analyzer to measure H₂O and CO₂ concentrations (Li-Cor LI-7500 Open path CO₂/H₂O Analyzer, LI-COR Inc.). The internal absolute pressure sensor of LI-7500 has a range of 150–1150 hPa with an accuracy of 1.5% of the full-scale span. The pressure port included in the enclosure guarantees that the internal pressure measured is representative of ambient conditions. The accuracy of the LI-7500 internal temperature sensor is 0.2 °C over a range of 0–70 °C. We positioned the internal sensor outside the control box to avoid artificial heating from surrounding electronic components.

For temperature, relative humidity and pressure measurements we also used a Delta OHM DO 9847 logger with Pt100 and Mk-33 sensors (Delta Ohm, DO9847 Multifunction meter).

Vaisala CARBOCAP® Carbon Dioxide Probe GMP343 was used to measure the CO₂ concentrations in the boundary layer (GMP343 Carbon Dioxide Probe for Demanding Measurements, Vaisala Oyj).

The Air Ion Spectrometer (AIS, AIREL Ltd., Estonia) measures the mobility distributions of both negative and positive air ions in the mobility range from 2.4 to 0.0075 cm² V⁻¹ s⁻¹ (Mirme *et al.* 2007). This corresponds to a diameter range of approximately 0.8 nm to 40 nm under conditions of 273 K and 1013 hPa. Since we carried out our measurements under different pressures, we corrected the mobilities accordingly (Tammet 1995, 1998). In essence, the AIS consists of two cylindrical aspiration type differential mobility analyzers (DMAs) equipped with insulated electrometer rings. Sampled ions are collected on the electrometer rings in 21 electrical mobility fractions simultaneously for both polarities. The time resolution for the AIS measurements was one minute.

We used adsorbent sampling to measure concentrations of several volatile organic compounds (VOC). Compounds were trapped into cartridges filled with Tenax-TA and Carboxen-B adsorbents. The adsorbent samples were analyzed using an automatic thermodesorption device connected to a gas chromatograph (HP-5890) and a mass spectrometer (HP-5972). Due to short sampling times, the sample volumes were below one liter, resulting in relatively large analytical uncertainties (Haapanala *et al.* 2006).

Modeling

Boundary layer modeling

We investigated whether the measured ion concentration profiles can provide information on the location of nucleation in the boundary layer by using the numerical boundary layer model SCADIS (Sogachev *et al.* 2002, 2004). The model is based on a one-and-a-half-order turbulence closure applying an $E-\omega$ scheme, where E is the turbulent kinetic energy and ω is the specific dissipation of E (Sogachev and Panferov 2006). The reader is referred to the above papers for details on model equations and numerical aspects.

Numerical simulations were carried out with the one-dimensional mode of SCADIS for the lower 3 km of the troposphere. The modeling domain was divided into 300 nodes with the vertical resolution decreasing exponentially from the surface towards the upper boundary. The area around Hyttiälä was assumed to be a forest with height 15 m, leaf area index 2 m² m⁻² and maximum of foliage at 2/3 height of the tree. The average measured wind speed during our measurements at the 70-m height was about 6 m s⁻¹. To get the same modeled wind speed at the 70-m height, we used the 10 m s⁻¹ geostrophic wind speed as the boundary condition for wind velocity in the model runs. Radiative forcing was provided by half-hour measurements interpolated at the model time step (20 s). We compared the modeled mixed layer height results with the balloon observations and SODAR-data from appropriate periods, and found a good agreement between the obtained heights.

In our modeling, we studied the profiles of

1.5–2 nm ions throughout the boundary layer. Instead of including aerosol dynamics, we used a rather conservative approach and treated particles as non-interacting tracer compounds. If the particles are formed at a certain boundary layer location (and we see an excess of charges based on the ion-DMPS data), all processes during the mixing lead negative ions towards equilibrium and thus decrease their concentration. Thus, in the real atmosphere, the differences between different altitudes should be more pronounced compared to those determined using our modeling approach.

For the chosen days, four locations of sources of particles were considered: (1) inside a 100-m thick layer just below the mixed layer top, which was indicated as turbulent kinetic energy $< 0.01 \text{ m}^2 \text{ s}^{-2}$, (2) inside a 100-m thick layer with the center at the eddy diffusivity maximum, (3) inside a 100-m thick layer adjacent to the ground surface, and (4) homogeneously throughout the whole mixed layer. All sources were assumed to have the same strength. In our model runs, we assumed that the sources were active only when incoming radiation exceeded 200 W m^{-2} . The simulated scalar fields were relaxed to zero with the relaxation time equal to one day. As boundary conditions we used the following: reflection of particles at lower (height = 0 m) and upper (height = 3 km) borders of the domain. Concentration profiles presented in the figure were normalized with the highest value of concentration within the mixed layer.

Results

Observations

We made observations during the spring 2005 (six flights) and spring 2006 (five flights). During the spring 2005 we were learning how to cope with contamination and measurement problems. We were also unlucky with nucleation events (there was not a single particle formation event during the campaign), so we present results from the spring 2006 only.

Table 1 shows the main characteristics of the five flight days for the spring 2006. All days were sunny and relatively cold. Condensable

organic vapour production rates (Haapanala *et al.* 2006) were around 60% lower than typical for this time of the year (Spanke *et al.* 2001, Spirig *et al.* 2004). Above the boundary layer (BL), concentrations were even lower; around half of those inside the BL.

10 March 2006

During this day, we had some technical problems with the AIS and we were not able to measure inside the mixed layer (ML), only in the residual layer (RL). Ground-based ion measurements showed a negative ion-induced nucleation episode below 3 nm lasting for six hours. However, for some reason, particles were not able to grow to sizes observable with DMPS. Nothing was seen for positive ions, so this was clearly an asymmetric nucleation event in favor of negative ions. Since we did not have 3 nm particles, ion-DMPS did not provide data for this day.

12 March 2006

There is a clear difference between negative and positive ions, indicating a negative ion-induced nucleation event lasting more than seven hours. We also saw a clear air mass change around 15:00. Before the air mass changed, some of the small particles were able to grow to sizes observable by the DMPS. Vertical ion profiles showed a clear difference: in the size range 2.5–3 nm there were hardly any positive ions, whereas the concentration of negative ions was increased. Larger sizes between 3 and 7 nm did not show such a sign differences. In the vertical aerosol particle number concentration, there was a sharp decrease from 4000 cm^{-3} inside the ML down to 700 cm^{-3} inside the RL.

Negative ions below 3 nm were well-mixed throughout the whole ML. If we consider the concentrations of 3–7 nm ions, we notice that negative ions were well-mixed, but positive ions had a clear maximum at the top of the BL. It is possible that this was an indication of ion-induced nucleation at the top of the BL: if negative ion-induced nucleation consumes most of negative cluster ions at the top of the BL, there

should be an excess of positive charges on the larger particles. During this day, the ion-DMPS showed a clear negative overcharging.

In addition to the ML nucleation, we saw new particle formation at the residual layer–free troposphere boundary as well.

13 March 2006

Our strongest particle formation day (Fig. 2) showed a clear difference between the negative and positive ion concentrations (Fig. 3). Negative 2 nm ions were seen for five hours, whereas positive ions were present for two hours only.

During this day, particles were negatively overcharged at the beginning and end of the nucleation burst (Fig. 4). Positive clusters were only slightly overcharged just before the negative population turned undercharged.

In the middle of the day, when the nucleation rates were at their highest, both negative and

positive particles were undercharged. This is an indication of a two-step process, where negative ions nucleate/activate with lower nucleating vapour concentrations than what is needed for homogeneous nucleation/neutral cluster activation (Fig. 4). The small positive overcharging near the period of strongest nucleation indicates that positive clusters may have been activated slightly before neutral activation/nucleation started.

The vertical profiles showed that the > 10 nm-particle concentration in the ML ($10\,000\text{ cm}^{-3}$) was approximately 100 times higher than that in the free troposphere (100 cm^{-3}) (Fig. 5). This indicates that nucleation took place inside the mixed layer. There was also a very clear sign-dependence in the profiles: the concentration of negative 1.5–2 nm ions was five-fold compared with positive ions (Fig. 6).

We could also observe an interesting two-fold structure, with a local minima at 250 m both for the concentration of 1.5–2 and 3–7 nm ions

Table 1. Basic characterization of flight days. Rows 1–5: basic meteorology. Rows 9 and 10: growth rates (GR) of negatively (–) and positively (+) charged particles in the diameter range of 1.3–3 nm. Row 11: sulphuric acid concentration calculated based on the method by Boy *et al.* (2005). Row 12: visual classification of the particle formation events according to Hirsikko *et al.* (2007). Row 13: the regions from where the air masses were coming from. Row 14: production rate of condensable organic vapours in the boundary layer (P) calculated using the method by Haapanala *et al.* (2006). Row 17: the maximum nucleation rate during the flight is based on the parameterization by Lovejoy *et al.* (2004).

	10 Mar. 2006	12 Mar. 2006	13 Mar. 2006	14 Mar. 2006	17 Mar. 2006
1 Temperature at 67 m (°C)	–10.7	–5.4	–0.8	–3.9	4.1
2 Global radiation (W m ^{–2})	336.6	279.2	346.0	396.6	207.9
3 Relative humidity (%)	78.3	65.3	56.4	65.0	54.2
4 Wind speed (m s ^{–1})	3.3	3.8	3.0	5.5	2.9
5 Wind direction (°)	48	51	71	122	271
6 Condensation sink $\times 10^3$ (s ^{–1})	5.27	2.33	2.39	3.14	1.89
7 [SO ₂] (ppb)	4.78	1.07	0.87	0.78	0.20
8 [NO _x] (ppb)	4.00	1.82	2.79	1.89	2.95
9 GR (–), 1.3–3 nm (nm h ^{–1})	–	1.6	1.8	1	–
10 GR (+), 1.3–3 nm (nm h ^{–1})	–	–	–	–	–
11 [H ₂ SO ₄] $\times 10^6$ (cm ^{–3})	2.9	2.1	2.6	2.0	0.8
12 BSMA event classification	lb.1	lb.1	I	lb.1	II
13 Origin of air mass	Baltic countries	Baltic countries	Belarus	S Russia	Baltic sea
14 $P \times 10^{-4}$ (cm ^{–3} s ^{–1})	0.5	0.4	0.7	1.4	0.7
15 Boundary layer height (m)	200	500	600	500	600
16 Residual layer (m)	200–600	500–1000	600–1200	500–900	600
17 BL negative ion-induced nucleation rate (cm ^{–3} s ^{–1})	7.9×10^{-3}	3.7×10^{-5}	3.3×10^{-5}	4.3×10^{-6}	2.3×10^{-6}
(maximum nucleation rate)	(1.8×10^{-1})	(5.9×10^{-3})	(3.5×10^{-3})	(1.1×10^{-3})	(1.1×10^{-3})
18 First decent	13:35–13:52	14:50–15:03	13:56–14:10	11:36–11:52	14:13–14:28
19 Second decent	14:00–14:16	15:10–15:20	14:20–14:30	12:00–12:10	14:44–14:54

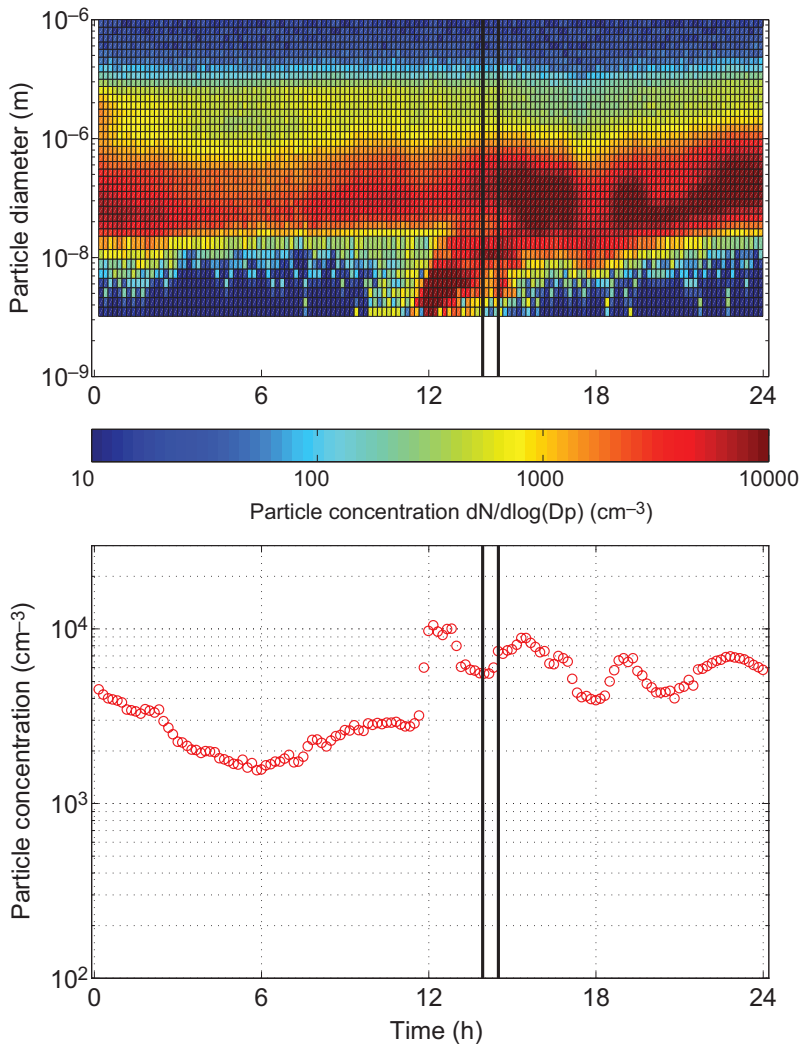


Fig. 2. Time evolution of the particle number size distribution and total number concentration measured by the DMPS at the SMEAR II station (ground-based) on 13 March 2006. The time of first descent with a balloon is indicated by a vertical black line.

(Fig. 7) during the first descent. This minimum clearly coincided with a small hump in the temperature profile (Fig. 8).

We also show observations from the SMEAR II station (the diamonds on the x -axes of Figs. 6, 7 and 8). Ground-based observations differed from balloon observations due to several reasons: (1) the particle concentration was rising rapidly from $\sim 3000 \text{ cm}^{-3}$ to $\sim 11\,000 \text{ cm}^{-3}$ during our flight, so that the average concentration over the whole flight period was smaller than the concentration at the end of the flight, (2) Uncertainties between the individual CPC's were $\pm 10\%$ (TSI, 2004) and between the AIS's $\pm 50\%$ (Vana *et al.* 2006), (3) the spatial distance from SMEAR II to the location of second descent was tens of kil-

ometers. Since the fluctuations in concentrations were high, this may naturally explain some part of the differences. Qualitatively, the measurements agreed well.

14 March 2006

As during previous days, we had a “bubble” of negative ions below 3 nm. However, particles were not able to grow above the detection limit of the DMPS. From the vertical ion profile, we could see that the concentration of 1.5–2 nm negative ions was much higher than that of positive ones. However, the concentration profiles were not as clear as during the earlier days. The

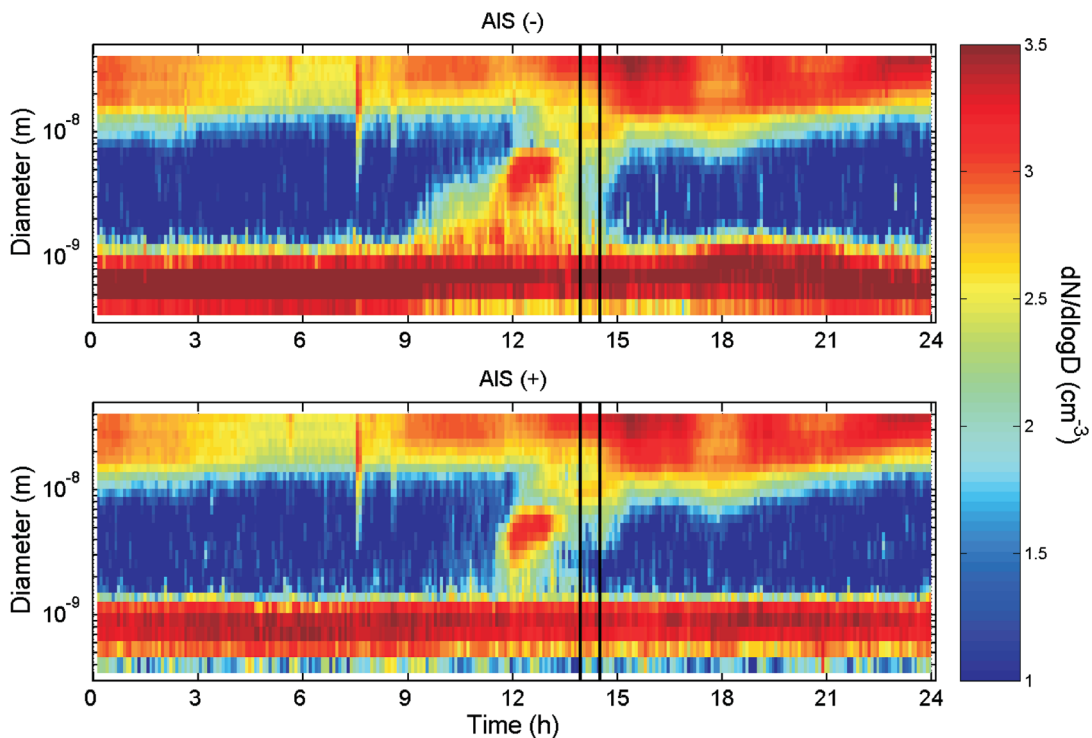


Fig. 3. Time evolution of the number size distribution of negative (top) and positive (bottom) ions measured by the AIS at the SMEAR II station (ground-based) on 13 March 2006. The time of first descent with a balloon is indicated by a vertical black line.

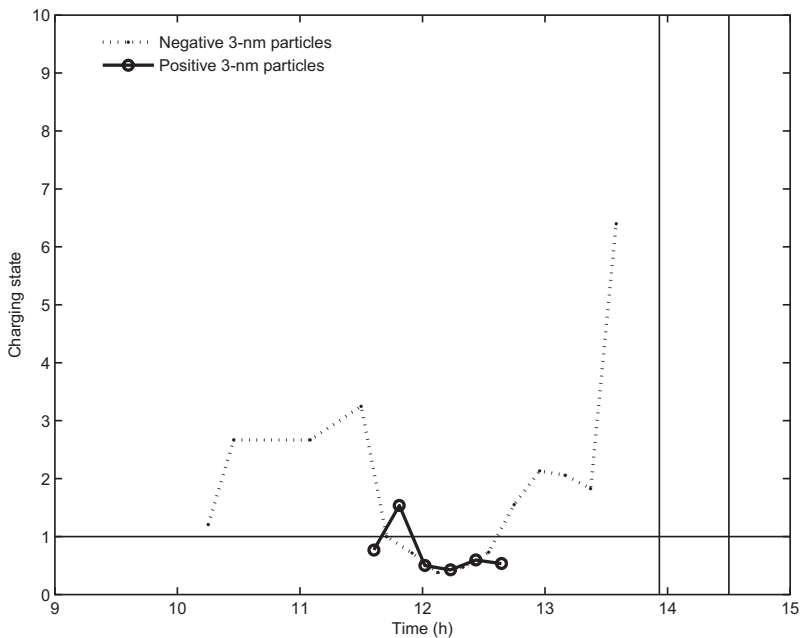


Fig. 4. Charging state of 3 nm particles (ground-based) on 13 March 2006. The time of first descent with a balloon is indicated by a vertical black line.

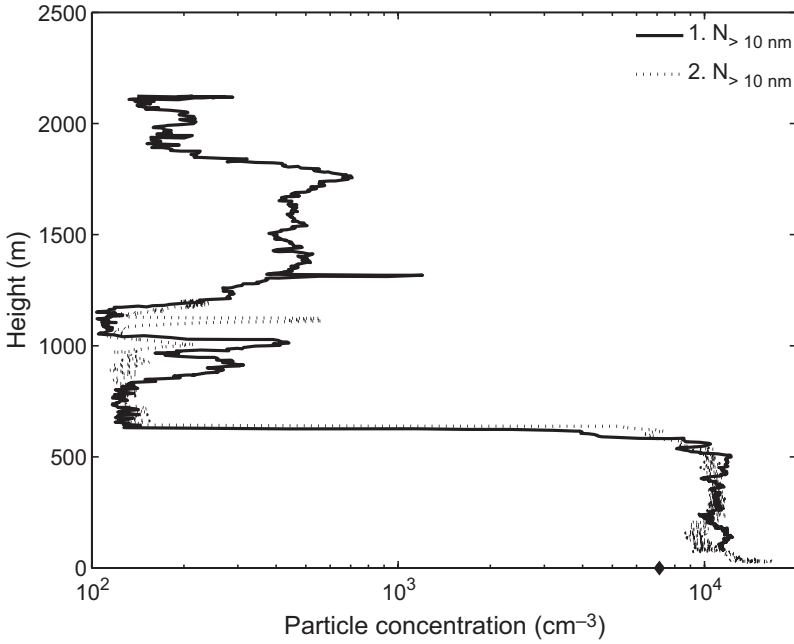


Fig. 5. Vertical profiles of the number concentration of > 10 nm particles on 13 March 2006. The numbers 1. and 2. refer to the first and second balloon decent, respectively.

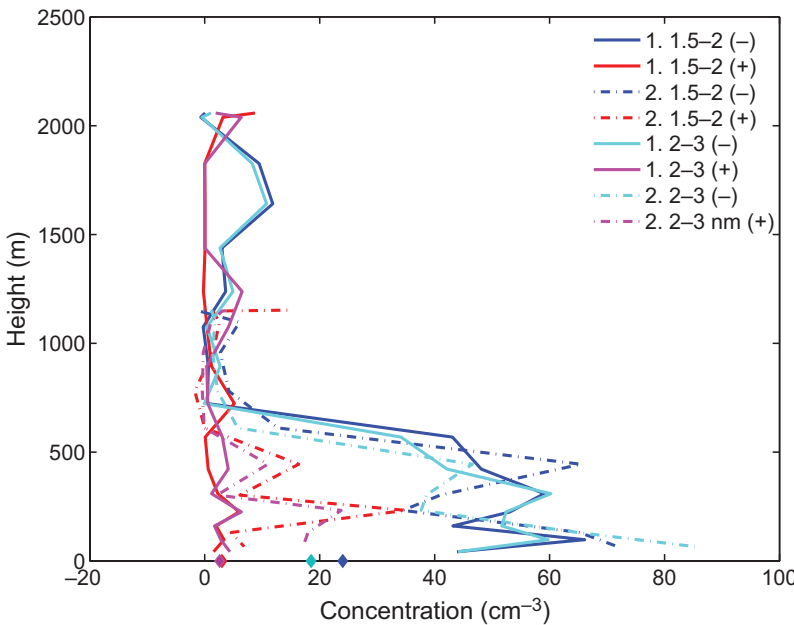


Fig. 6. Vertical profiles of the number concentrations of negative and positive ions in size ranges 1.5–2 and 2–3 nm on 13 March 2006. Numbers 1 and 2 refer to the first and second balloon decent, respectively.

concentration maxima for the 1.5–2 nm and 3–7 nm ions occurred at the height of 300 m, which again coincided with the changes in the temperature profile. No clear profile could be seen for > 10 nm particle number concentrations. For this day, the 3 nm particle number concentration was so low that we can not say anything about the charging state of the particles. During this day,

we also observed nucleation in the residual layer, separate from the mixed layer.

17 March 2006

This day featured only a small “bubble” of negative 2–5 nm ions. However, another interest-

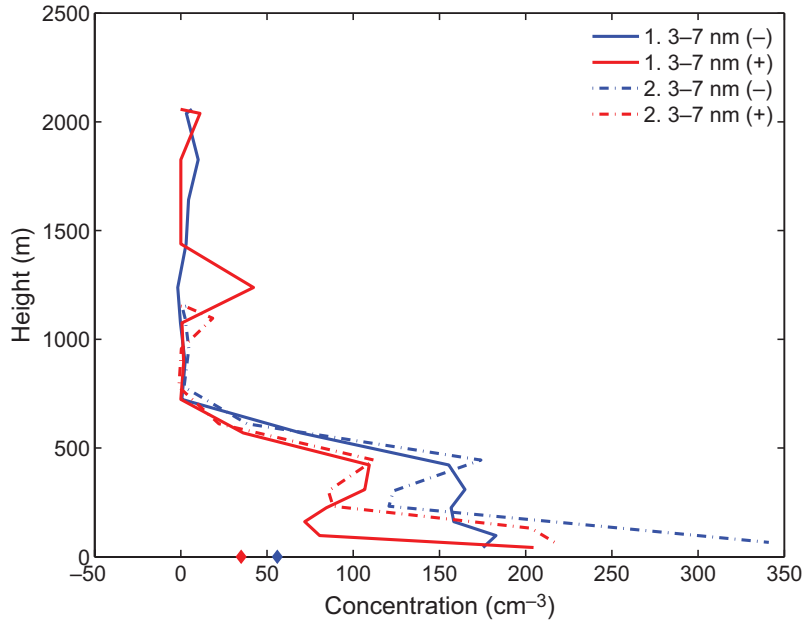


Fig. 7. Vertical profiles of the number concentration of negative and positive 3–7 nm ions on 13 March 2006. Numbers 1 and 2 refer to the first and second balloon decent, respectively.

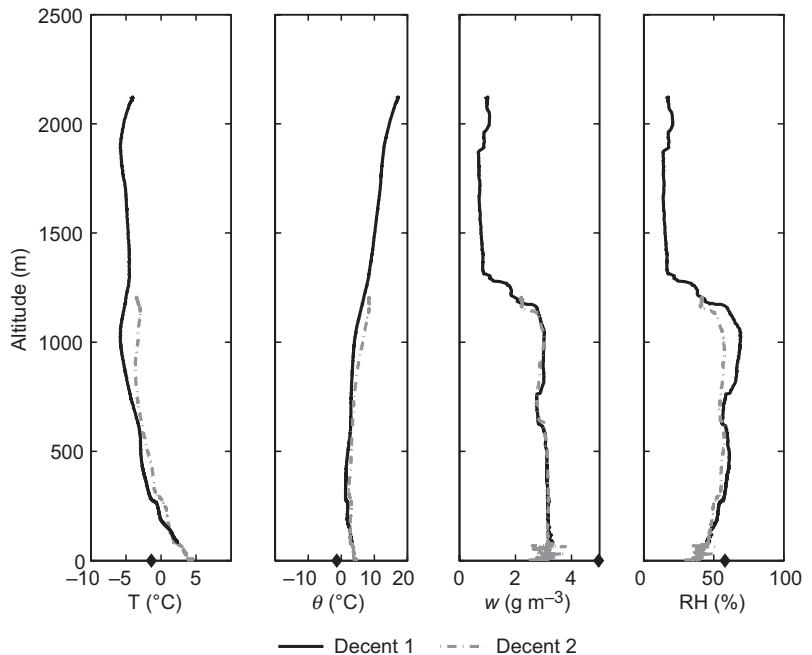


Fig. 8. Profiles of meteorological variables on 13 March 2006.

ing phenomenon appeared: small negative ions exhibited a concentration maximum above the BL. Since this was observed on only one day, we can not draw any reliable conclusions. However, based on the increase in water vapour and the presence of some ice crystals, we suppose that the observations may be somehow related to

ions produced by water or ice crystal interactions (Hörrak *et al.* 2005, Hirsikko *et al.* 2007). For this day, the 3 nm particle concentration is so low that we can not say anything about the charging state of the particles based on ion-DMPS data.

The summary of vertical 1.5–3 nm ion profiles are given in Fig. 9.

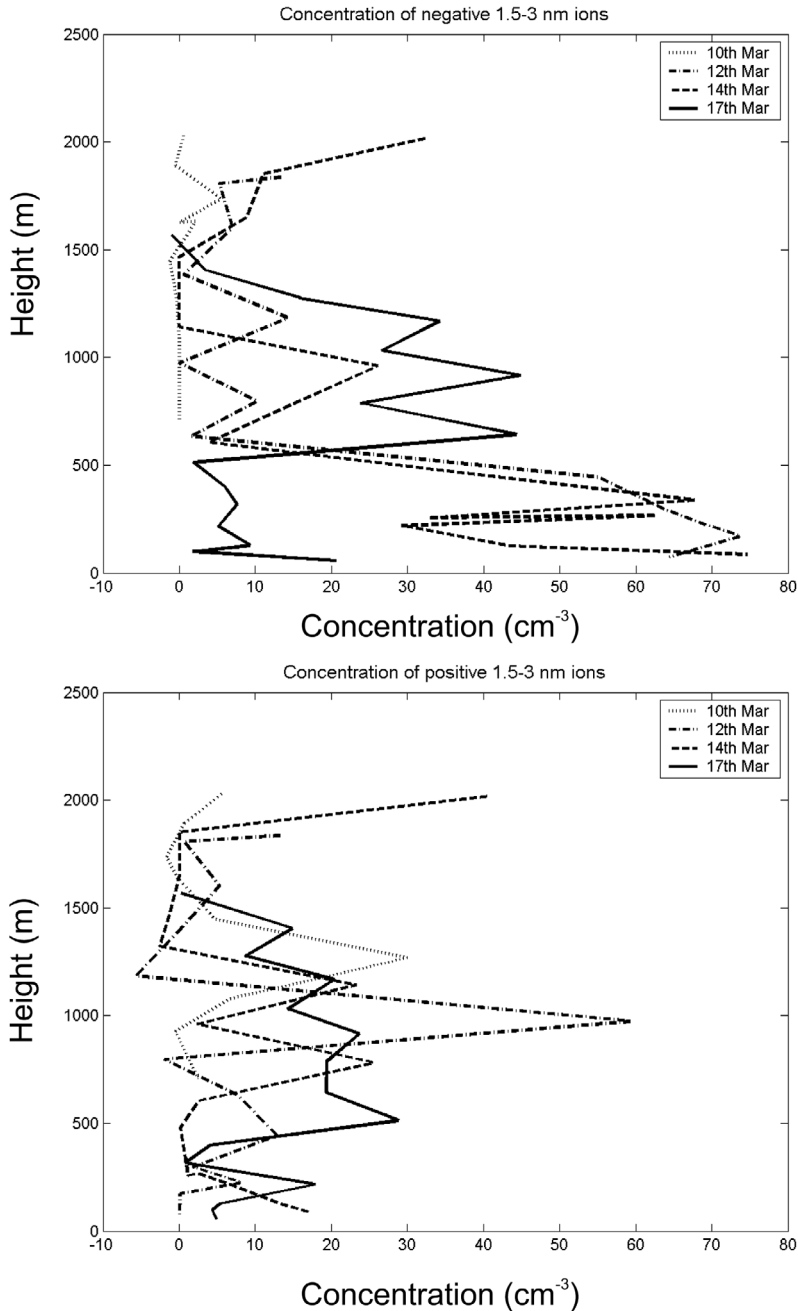


Fig. 9. Vertical profiles of the number concentrations of negative (top) and positive (bottom) ions in the size range 1.5–3 nm on 10, 12, 14 and 17 March 2006.

Modeling results

Comparison with ion-induced nucleation theories

As the best existing theory on ion-induced nucleation is based on the work by Lovejoy *et al.* (2004), we followed their method to interpret our

profiles. We instantly notice that during all of our days, binary water-sulphuric acid ion-induced nucleation calculated from the theory of Lovejoy *et al.* (2004) was not able to explain our results (*see* Table 1). On 10 March 2006, the maximum negative ion-induced nucleation rate inside the BL was smaller than $10^{-2} \text{ cm}^{-3} \text{ s}^{-1}$. During all other days, it was smaller than $10^{-4} \text{ cm}^{-3} \text{ s}^{-1}$. We

also varied sulphuric acid concentrations calculated with the method described by Boy *et al.* (2005) to account for possible inaccuracies in investigations. Even after doubling the sulphuric acid concentration, we were much below the limit where binary ion-induced nucleation would be able to explain the observations, except for 10 March 2006. Thus, clusters may have been stabilized by some other compounds as suggested by Lovejoy *et al.* (2004).

Recent quantum chemical computations by Kurtén *et al.* (2007) indicate that the stabilizing species may be some other than the often-suggested candidate ammonia, since it is only very weakly bound to the HSO_4^- ion. This can be explained by acid-base chemistry: NH_3 , a moderately strong base, is much more attracted to the strong acid H_2SO_4 than to the weak acid HSO_4^- . Also, the presence of ammonia did not increase the water affinity of $(\text{HSO}_4^-) \cdot (\text{H}_2\text{O})_x$ clusters. These findings imply that ammonia is unlikely to stabilize small negatively-charged clusters. It is possible that ammonia may enhance the growth of some $(\text{HSO}_4^-) \cdot (\text{H}_2\text{SO}_4)_y(\text{H}_2\text{O})_x$ clusters in the sulphuric acid co-ordinate, as was recently demonstrated for neutral $(\text{H}_2\text{SO}_4)_2(\text{H}_2\text{O})_x$ clusters by L. Torpo (unpubl. data). However, such an enhancement would then be caused only by the ammonia–neutral acid interactions, with the core ion playing no role. Thus, the nucleation-enhancing effect of ammonia on negatively charged clusters can maximally be as large as that observed for neutral clusters, and is probably much less. If some compound indeed does stabilize the HSO_4^- -based clusters, as predicted by Lovejoy *et al.* (2004), it is therefore likely to be some organic vapour rather than ammonia.

The low levels of positive ion-induced nucleation in the sulphuric acid–water system are probably explained by simple acid-base chemistry. Positive charges in atmospheric chemical systems are usually localized on protons (H^+). Sulphuric acid, as a strong acid, is a strong proton donor and very poor proton acceptor. In other words, the binding of sulphuric acid to clusters containing extra protons is very unfavorable thermodynamically. If sulphuric acid does bind to positively charged clusters, it is despite, not because of the presence of excess protons. Thus, it is not surprising that the sulphuric acid con-

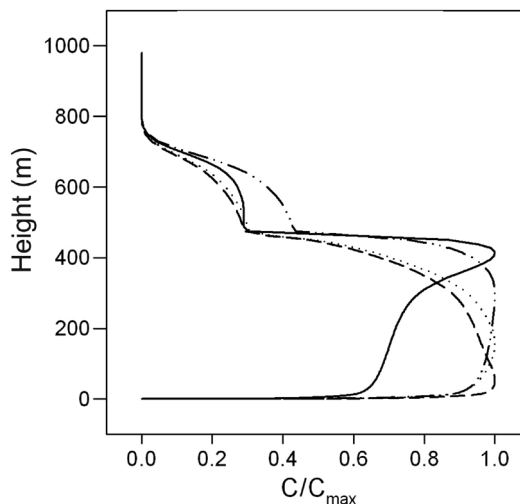


Fig. 10. Vertical profiles of cluster concentrations (scaled with respect to the maximum concentrations) on 13 March 2006 by assuming that nucleation takes place at different parts of the boundary layer (solid line: ABL top; dotted line: nucleation at eddy maximum; dashed line: nucleation on the surface; dash-dotted line: uniform source through the whole BL).

centration required for the onset of positive ion-induced nucleation is not lower than that required for activation of possible neutral clusters.

Estimates on location of nucleation

Figure 10 shows different cluster profiles resulting from nucleation taking place at different locations in the boundary layer calculated for 13 March 2006. Typically, upward mixing is faster than downward mixing. We can see that if nucleation takes place in the uppermost 100 meters of the BL, the profile is significantly different as compared with that for the three other cases. For all of our five days, the profiles do not look like the case where nucleation takes place at the top of the boundary layer.

We can also compare our results with the calculation carried out by Boy *et al.* (2006). Boy and co-authors calculated with the one-dimensional model MALTE the vertical structure of newly formed particles in two size ranges (1–3 and 3–6 nm). The simulations indicated a maximum concentration of small clusters at the ground level in the morning. Around noon, these

clusters had grown to the detectable size range of 3–6 nm, and were nearly equally mixed inside the mixed layer. Their results agreed qualitatively with measured vertical profiles reported by O'Dowd *et al.* (2005) for the same day. One should, however, keep in mind that there is much variability, and that this agreement is true only for single profile.

The relation between ground-based and flight observations

When we compare ion-concentration distributions at different heights measured using the hot-air balloon and the corresponding ground based measurements at the SMEAR II station, we notice that the size distributions are pretty similar to each other. However, our balloon-borne CPC showed somewhat higher total number concentrations than the SMEAR-DMPS. The effect is not due to contamination, since the difference was systematically around 50%, regardless of particle concentrations in the concentration interval 100–10 000 cm⁻³. This might in practice be due to different CPCs and different ambient conditions for measurements. Thus, the number concentrations and size distributions behave in similar ways, and we can actually use surface observations to investigate atmospheric nucleation phenomena.

Conclusions

We observed boundary layer profiles for particles, ions and meteorological data during several nucleation event days in a boreal forest. The observations showed that the particle formation observed at the surface was relatively homogeneous throughout the whole boundary layer. However, we also observed separate particle formation inside the residual layer during one day, which is in agreement with earlier observations by Stratmann *et al.* (2003). Particle concentration profiles from the mixed layer showed that surface measurements usually represent concentrations throughout the mixed layer relatively well.

During our measurements, there was a clear difference between negative and positive ions:

the concentrations of negative 1.5–2 nm ions were several times larger than those of positive ions throughout the mixed layer. This is a clear indication of ion-induced nucleation, in which negative ions played a significant role. In addition to that, also neutral nucleation/activation was important.

On 13 March 2006, combined data from the balloon and surface measurements showed that at the onset and end of the nucleation event, negative ions activated and the particle population was negatively overcharged. In the middle of the burst, also positive and neutral clusters started to activate, or neutral homogeneous nucleation started.

We also noticed that during several days, the activation of small negative ions without growth to sizes observable with DMPS occurred. We suppose that the reason for the lack of growth was low organic vapour concentrations (Haapanala *et al.* 2006). Recently, it was shown that organic vapours are needed to make the particle growth rapid enough (Kulmala *et al.* 2004b).

If we assume that sulphuric acid plays an important role in new-particle formation, the qualitative differences between negative, and positive and neutral nucleation can be related to simple acid-base chemistry. Recent quantum chemical calculations support this analysis (Kurtén *et al.* 2007). However, these calculations also indicate that ammonia is unlikely to stabilize small negatively-charged water–sulphuric acid clusters. When we calculated the negative ion-induced nucleation rates based on the method by Lovejoy *et al.* (2004), we noticed that pure water–sulphuric acid nucleation is not able to explain the results without assuming some additional stabilizing component as suggested in that article.

To investigate the potential location of nucleation, we carried out boundary layer mixing simulations assuming that nucleation takes place in four different locations. Based on these results, we assume that nucleation did not take place at the top of mixed layer, but rather throughout the layer.

As a final conclusion, our measurements showed that a hot-air balloon is a suitable platform for boundary layer measurements, and it can be used to observe ion dynamics and particle formation.

Acknowledgements: The study was in part supported by the Academy of Finland and the Nessling Foundation. Thanks are due to Markku Sipinen and Reijo Lampinen from Aero-naut ballooning company, Tikkakoski, Finland for the bal-loon flights. We are grateful to Taina Ruuskanen, Erkki Siivola, Heikki Laakso and Andreas Kürten for their practical help with the measurements.

References

- Boy M., Kulmala M., Ruuskanen T.M., Pihlatie M., Reis-sell A., Aalto P.P., Keronen P., Dal Maso M., Hellen H., Hakola H., Jansson R., Hanke M. & Arnold F. 2005. Sul-phuric acid closure and contribution to nucleation mode particle growth. *Atmos. Chem. Phys.* 5: 863–878.
- Boy M., Hellmuth O., Korhonen H., Nilsson E. D., ReV-elle D., Turnipseed A., Arnold F. & Kulmala M. 2006. MALTE — model to predict new aerosol formation in the lower troposphere. *Atmos. Chem. Phys.* 6: 4499–4517.
- Haapanala S., Rinne J., Hakola H., Hellén H., Laakso L., Lihavainen H., Janson R. & Kulmala M. 2006. Bound-ary layer concentrations and landscape scale emissions of volatile organic compounds in early spring. *Atmos. Chem. Phys. Discuss.* 6: 10567–10589.
- Hari P. & Kulmala M. 2005. Station for Measuring Ecosys-tem–Atmosphere Relations (SMEAR II). *Boreal Env. Res.* 10: 315–322.
- Hellmuth O. 2006a. Columnar modelling of nucleation burst evolution in the convective boundary layer — first results from a feasibility study. Part I: Modelling approach. *Atmos. Chem. Phys.* 6: 4175–4214.
- Hellmuth O. 2006b. Columnar modelling of nucleation burst evolution in the convective boundary layer — first results from a feasibility study. Part II: Meteorological characterization. *Atmos. Chem. Phys.* 6: 4215–4230.
- Hellmuth O. 2006c. Columnar modelling of nucleation burst evolution in the convective boundary layer — first results from a feasibility study. Part III: Preliminary results on physicochemical model performance using two “clean air mass” reference scenarios. *Atmos. Chem. Phys.* 6: 4231–4251.
- Hellmuth O. 2006d. Columnar modelling of nucleation burst evolution in the convective boundary layer — first results from a feasibility study. Part IV: A compilation of previous observations for valuation of simulation results from a columnar modelling study. *Atmos. Chem. Phys.* 6: 4253–4274.
- Hirsikko A., Bergman T., Laakso L., Dal Maso M., Riipinen I., Hörrak U. & Kulmala M. 2007. Identification and classification of the formation of intermediate ions mea-sured in boreal forest. *Atmos. Chem. Phys.* 7: 201–210.
- Hoppel W.A., Frick G.M., Fitzgerald J.W. & Larsson R.E. 1994. Marine boundary layer measurements of new par-ticle formation and the effects nonprecipitating clouds have on aerosol size distributions. *J. Geophys. Res.* 99: 14443–14459.
- Hoppel W., Fitzgerald J., Frick G., Caffrey P., Pasternack L., Hegg D., Gao S., Leaitch R., Shantz N., Cantrell C., Albrechtski T., Ambrusko J. & Sullivan W. 2001. Par-ticle formation and growth from ozonolysis of α -pinene. *J. Geophys. Res.* 106: 27603–27618.
- Hörrak U., Tammet H., Aalto P.P., Vana M., Hirsikko A., Laakso L. & Kulmala M. 2005. Formation of charged nanometer aerosol particles associated with rainfall. In: Maenhaut W. (ed.), *Abstracts of the European Aerosol Conference 2005*, Ghent, Belgium, 28 August–2 Sep-tember 2005, p. 606.
- Hyvönen S., Junninen H., Laakso L., Dal Maso M., Grön-holm T., Bonn B., Keronen P., Aalto P., Hiltunen V., Pohja T., Launiainen S., Hari P., Mannila H. & Kulmala M. 2005. A look at aerosol formation using data mining techniques. *Atmos. Chem. Phys.* 5: 3345–3356.
- Kerminen V.-M., Pirjola L. & Kulmala M. 2001. How significantly does coagulative scavenging limit atmospheric particle production? *J. Geophys. Res.* 106: 24119–24126.
- Kulmala M. 2003. How particles nucleate and grow. *Science* 302: 1000–1001.
- Kulmala M., Pirjola L. & Mäkelä J.M. 2000. Stable sulphate clusters as a source of new atmospheric particles. *Nature* 404: 66–69.
- Kulmala M., Lehtinen K.E.J. & Laaksonen A. 2006. Clus-ter activation theory as an explanation of the linear dependence between formation rate of 3 nm particles and sulphuric acid concentration. *Atmos. Chem. Phys.* 6: 787–793.
- Kulmala M., Vehkamäki H., Petäjä T., Dal Maso M., Lauri A., Kerminen V.-M., Birmili W. & McMurry P.H. 2004a. Formation and growth rates of ultrafine atmospheric particles: a review of observations. *J. Aerosol Sci.* 35: 143–176.
- Kulmala M., Laakso L., Lehtinen K.E.J., Riipinen I., Dal Maso M., Anttila T., Kerminen V.-M., Hörrak U., Vana M. & Tammet H. 2004b. Initial steps of aerosol growth. *Atmos. Chem. Phys.* 4: 2553–2560.
- Kulmala M., Hämeri K., Aalto P.P., Mäkelä J.M., Pirjola L., Nilsson E.D., Buzorius G., Rannik Ü., Dal Maso M., Seidl W., Hoffmann T., Janson R., Hansson H.-C., Viisanen Y., Laaksonen A. & O’Dowd C.D. 2001. Over-view of the international project on biogenic aerosol formation in the boreal forest (BIOFOR). *Tellus* 53B: 324–343.
- Kürtén T., Noppel M., Vehkamäki H., Salonen M. & Kul-mala M. 2007. Quantum chemical studies of hydrate formation of H_2SO_4 and HSO_4^- . *Boreal Env. Res.* 12: 431–453.
- Laakso L., Gagné S., Petäjä T., Hirsikko A., Aalto P.P., Kul-mala M. & Kerminen V.-M. 2007. Detecting charging state of ultra-fine particles: instrumental development and ambient measurements. *Atmos. Chem. Phys.* 7: 1333–1345.
- Lovejoy E.R., Curtius J. & Froyd K.D. 2004 Atmospheric ion-induced nucleation of sulfuric acid and water. *J. Geo-phys. Res.* 109, D08204, doi:10.1029/2003JD004460.
- Mirme A., Tamm E., Mordas G., Vana M., Uin J., Mirme S., Bernotas T., Laakso L., Hirsikko A. & Kulmala M. 2007. A wide-range multi-channel Air Ion Spectrometer.

- Boreal Env. Res.* 12: 247–264.
- Nilsson E.D., Rannik Ü, Kulmala M., Buzorius G. & O'Dowd C.D. 2001. Effects of the continental boundary layer evolution, convection, turbulence and entrainment on aerosol formation. *Tellus* 53B: 441–461.
- Nilsson E.D. & Kulmala M. 1998. The potential for atmospheric mixing processes to enhance the binary nucleation rate. *J. Geophys. Res.* 103: 1381–1389.
- O'Dowd C.D., Yoon Y.J., Junkermann W., Aalto P.P. & Lihavainen H. 2005. Airborne measurements of nucleation mode particles, II: boreal forest events. *Report Series in Aerosol Science* 76: 162–173.
- Siebert H., Stratmann F. & Wehner B. 2004. First observations of increased ultrafine particle number concentrations near the inversion of a planetary boundary layer and its relation to ground-based measurements. *Geophys. Res. Lett.* 31, L09102, doi:10.1029/2003GL019086.
- Sogachev A., Menzhulin G., Heimann M. & Lloyd J. 2002. A simple three-dimensional canopy–planetary boundary layer simulation model for scalar concentrations and fluxes. *Tellus* 54B: 784–819.
- Sogachev A., Rannik Ü. & Vesala T. 2004. On flux footprints over the complex terrain covered by a heterogeneous forest. *Agric. For. Meteorol.* 127: 143–158.
- Sogachev A. & Panferov O. 2006. Modification of two-equation models to account for plant drag. *Boundary Layer Meteorol.* 121: 229–266.
- Spanke J., Rannik Ü., Forkel R., Nigge W. & Hoffmann T. 2001. Emission fluxes and atmospheric degradation of monoterpenes above a boreal forest: field measurements and modelling. *Tellus B* 53: 406–422.
- Spirig C., Guenther A., Greenberg J.P., Calanca P. & Tarvainen V. 2004. Tethered balloon measurements of biogenic volatile organic compounds at a Boreal forest site. *Atmos. Chem. Phys.* 4: 215–229.
- Stratmann F., Siebert H., Spindler G., Wehner B., Althausen D., Heinzenberg J., Hellmuth O., Rinke R., Schmiedler U., Seidel C., Tuch T., Uhrner U., Wiedensohler A., Wandinger U., Wendisch M., Schell D. & Stohl A. 2003. New-particle formation events in a continental boundary layer: first results from the SATURN experiment. *Atmos. Chem. Phys.* 3: 1445–1459.
- Stull R.B. 1988. *An introduction to boundary layer meteorology*. Kluwer Academic Publishers, Dordrecht.
- Tammet H. 1995. Size and mobility of nanometer particles, clusters and ions. *J. Aerosol Sci.* 26: 459–475.
- Tammet H. 1998. Reduction of air ion mobility to standard conditions. *J. Geophys. Res.* 103: 13933–139.
- Vana M., Mordas G., Mirme A. & Kulmala M. 2006. Calibration and data evaluation of the Air Ion Spectrometer, comparison with the Balanced Scanning Mobility Analyser. *Report Series in Aerosol Science* 81B: 634–638.